Synthesis and Biological Evaluation of a Fluorine-18 Derivative of Dasatinib

Darren R. Veach,[†,‡] Mohammad Namavari,[‡,§] Nagavarakishore Pillarsetty,[†,‡] Elmer B. Santos,[‡] Tatiana Beresten-Kochetkov,[†] Caryl Lambek,[†] Blesida J. Punzalan,[‡] Christophe Antczak,[†,#] Peter M. Smith-Jones,[†,‡] Hakim Djaballah,[†,#] Bayard Clarkson,[†] and Steven M. Larson*[,†,‡]

Department of Molecular Pharmacology and Chemistry and Department of Radiology, Memorial Sloan-Kettering Cancer Center, 1275 York Avenue, New York, New York 10021

Received March 23, 2007

Tyrosine kinases often play pivotal roles in the pathogenesis of cancer and are good candidates for therapeutic intervention and targeted molecular imaging. The precursor synthesis, radiosynthesis, and biological characterization of a fluorine-18 analog of dasatinib, a multitargeted kinase inhibitor, are reported. Compound **5** potently inhibits Abl, Src, and Kit kinases and inhibits K562 and M07e/p210$^{bcr-abl}$ human leukemic cell growth. Using positron emission tomography, we visualized K562 tumor xenografts in mice with [^{18}F]-**5**.

Introduction

A central focus of modern medicine is to develop care that is highly individualized to each patient. An important facet of this has been kinase inhibitor therapy, and signal transduction modulation in general is revolutionizing disease treatment. Another key aspect of customized care is obtaining a detailed disease profile through noninvasive medical imaging techniques such as positron emission tomography (PET[a]) and using this to assess disease status and determine the optimal course of treatment. Molecular and functional imaging with radiotracers such as [^{18}F]-fluoro-2-deoxy-D-glucose (FDG) and [^{18}F]-3′-deoxy-3′-fluorothymidine (FLT) are particularly useful as surrogate markers in cancer diagnosis and management.[1,2] However, more sophisticated tumoral information is necessary to predict response or observe the onset of drug resistance. Radiolabeled small molecule imaging modalities that are matched to a given kinase inhibitor and are capable of querying a specific molecular target are one solution, potentially. Here, we describe the synthesis, in vitro, and preliminary in vivo micro-PET imaging of one such kinase-directed probe, a fluorine-18 derivative of dasatinib.

Our focus is the development of PET radiotracers targeting Abl, Src, Kit, and other kinases relevant to cancer. Normal Abl and Src kinases are expressed in a variety of tissues and are tightly regulated and inactive most of the time. Both have many functions and associations in vivo, but generally, Src regulates cell adhesion and motility, while Abl is involved in cytoskeletal reorganization[3] and cell death signaling.[4] In some leukemias, a reciprocal t(9;22) translocation between the ABL and BCR genes forms the Philadelphia chromosome (Ph), whose mutant gene product, Bcr-Abl, is a constitutively activated tyrosine kinase. Bcr-Abl causes chronic myelogenous leukemia (CML) and some types of acute lymphoblastic leukemia (ALL).[5] Src tyrosine kinase is activated and overexpressed in numerous malignancies, mutated in a few examples, and is often associated with increased motility, invasiveness, or metastasis in cancer.[6] The abundance, activation, and disregulation of Bcr-Abl and Src in cancer have made these kinases attractive targets for drug development and, more recently, molecular imaging.

Imatinib (**1**), a Bcr-Abl tyrosine kinase inhibitor, is one of the most well-known molecularly targeted therapeutics and has revolutionized treatment of CML.[7,8] Imatinib is also approved for gastrointestinal stromal tumor (GIST) therapy and acts via inhibition of c-Kit receptor tyrosine kinase.[9] While imatinib has been a major breakthrough, resistance to kinase inhibitor therapy arises from a number of mechanisms including kinase-domain point mutations (pre-existing or acquired), upregulation of Bcr-Abl, activation of alternate, compensatory kinase pathways (Src family), and drug transporters.[10] These issues have fueled the development of a number of next-generation Bcr-Abl inhibitors.[11,12] Dasatinib (BMS-354825, **2**) is a high affinity dual Src/Abl and c-Kit inhibitor recently approved for all categories of imatinib-refractory CML and Ph+ ALL.[13,14] Dasatinib is effective in many imatinib resistant Bcr-Abl kinase domain mutants, but the "gatekeeper" mutants like T315I or F317L remain problematic.[14]

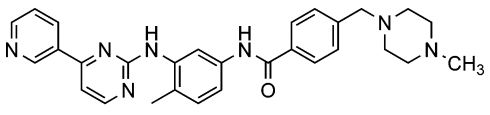

1 (imatinib)

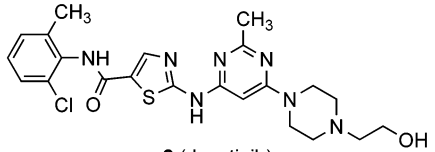

2 (dasatinib)

^{14}C- and ^{3}H-labeled (beta-emitting) radiotracers are produced routinely in drug development, but kinase inhibitors bearing positron-emitting isotopes are much less developed. No kinase inhibitor-based imaging probe exists yet for routine use in humans, though the number of promising kinase-targeted PET radiotracers is growing rapidly. Thus far, the majority of effort

* To whom correspondence should be addressed. Phone: (212) 639-7373. Fax: (212) 717-3263. E-mail: larsonS@mskcc.org.
† Department of Molecular Pharmacology and Chemistry.
‡ Department of Radiology.
§ Current address: Multimodality Molecular Imaging Lab, Department of Radiology, Stanford University, School of Medicine, Stanford, CA 94305.
# High Throughput Screening Facility, Memorial Sloan-Kettering Cancer Center, New York, NY 10021.

[a] Abbreviations: ALL, acute lymphoblastic leukemia; CML, chronic myelogenous leukemia; FDG, [^{18}F]-fluoro-2-deoxy-D-glucose; FLT, [^{18}F]-3′-deoxy-3′-fluorothymidine; GIST, gastrointestinal stromal tumor; PET, positron emission tomography; Ph, Philadelphia chromosome.

10.1021/jm070342g CCC: $37.00
Published on Web 10/23/2007

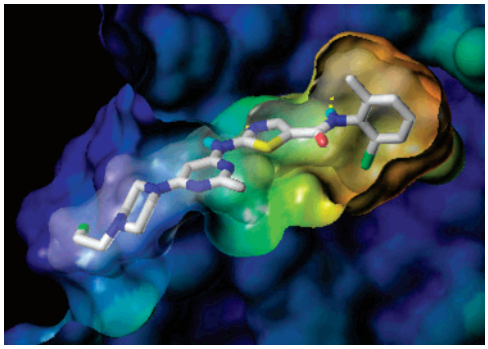

Figure 1. Cavity depth Connolly surface rendering of **5** docked into Abl kinase domain.

has been by vanBrocklin, Mishani, and others on quinazoline-type small-molecule probes for EGFR tyrosine kinase, which is overexpressed in some cancers.[15−17] More recently, Wang et al. reported the synthesis of [^{11}C]-gefitinib[18] and [^{18}F]-sunitinib.[19]

At first, perhaps hematopoietic disorders, like CML, may not seem like logical imaging targets due to their peripheral nature, but imaging hyperproliferation in bone marrow has been known for some time.[20,21] Recently, [^{18}F]-FLT PET was used to clearly distinguish bone marrow in patients with myeloproliferative disorders from normal.[22] [^{11}C]-AG957 was the first example of a Bcr-Abl-targeted radiotracer specifically developed for PET, but this tracer suffers from inherent chemical instability and weak target binding relative to newer inhibitors.[23] Our group has reported an [^{124}I]-pyridopyrimidinone derivative,[24] which binds tightly to Bcr-Abl, among other kinases, but does not possess an ideal logP. Recently, the Fowler group reported [^{11}C]-imatinib, which was imaged in baboon.[25] Generally, ^{18}F is more convenient for PET imaging studies, as it has a 110-minute half-life, unlike ^{11}C ($T_{1/2}$ = 20 min).

When considering the structure of dasatinib, the hydroxyethylpiperazinyl moiety was ideal for derivatization based on binding orientation. Chemically, the most straightforward approach conveniently was at the same site; *N*-alkylation of the unsubstituted piperazine with a simple fluorine-containing group or activated precursor for fluoride displacement.[26] Thus, we endeavored to construct an analog of dasatinib bearing an [^{18}F] fluoroethyl substituent. *N*-(2-Fluoroethyl)piperazines are not widely reported, but Katzenellenbogen and Welch described a successful synthesis of activated ethylpiperazines and subsequent displacement with ^{18}F.[27] Sterically, hydroxyl-to-fluoro substitution is tolerated well, so long as the hydroxyl is not involved in critical H-bonding. Prior experience with pyridopyrimidinone Src/Abl inhibitors[28] and molecular docking studies into the Abl crystal structure predicted that the dasatinib pharmacophore would share much of the same binding characteristics in which an arene sits deep within the catalytic pocket and the substitutents on N4 of the piperazine would protrude from a solvent accessible hole in the kinase catalytic domain (Figure 1).

Results and Discussion

Synthesis. The synthesis of both ^{18}F radiotracer and ^{19}F reference analogs began with chloropyrimidine **3**, an intermediate that was synthesized according to the literature.[13] An S_NAr displacement with piperazine gave compound **4** in good yield (78%). The 2-fluoroethyl reference compound **5** was obtained by alkylation of **4** with 1-bromo-2-fluoroethane in the presence of Na_2CO_3 and catalytic KI (Scheme 1).

Radiosynthesis. We envisioned that the best way to arrive at the [^{18}F]-*N*-2-fluoroethyl-labeled compound was a two-step process in which a two-carbon synthon containing two leaving groups was displaced with F-18 first, then reacted with piperazine **4**. A one-step radiosynthesis would be ideal, however, we feared that intramolecular cyclization would be a problematic competing reaction in a precursor containing a X−CH_2CH_2−NR_2 system—a piperazine beta to a leaving group that is significantly reactive with fluoride ion.

Scheme 1. Synthesis of an Unlabeled (^{19}F) Fluorinated Derivative of Dasatinib[a]

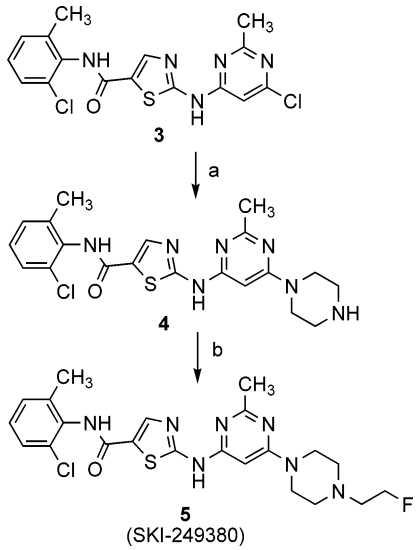

[a] Reagents and conditions: (a) piperazine, diisopropyl-ethylamine, dioxane, reflux, 12 h, 78%; (b) 1-bromo-2-fluoroethane, Na_2CO_3, KI, CH_3CN, 60 °C, 4 h, 84%.

In this study, it was found that either trifluoromethanesulfonate or *p*-toluenesulfonate precursors worked. 2-Bromoethyl triflate, **6**, has been used to install a [^{18}F]-fluoroethyl moiety on piperazines before and is easily obtained by triflation of 2-bromoethanol and triflic anhydride.[27] Precursor **6** was treated with [^{18}F]-KF/Kryptofix 2.2.2 to form [^{18}F]-1-bromo-2-fluoroethane, **7**. The decay-corrected radiochemical yield of the *N*-alkylation step was 25.1 ± 5.8%. Overall, a 6.6 ± 2.3% yield was obtained from starting fluoride. The specific activity was 29.7 ± 9.7 mCi/μmol (n = 3). These conditions were optimized and it was found that [^{18}F]-**7** could be distilled rapidly prior to the alkylation of **4**, which improved yields of [^{18}F]-**5** somewhat to 9.8 ± 5.0%. The average specific activity improved considerably to 2560 mCi/μmol (n = 11, range 108−7350 mCi/μmol). The low yield could be a result of complications due to hydrolysis or volatility of **6** or **7**. To address this problem, we examined a less labile, less volatile alternative. [^{18}F]-2-fluoroethyl tosylate, **8**, is generated in situ in a similar fashion from ethylene glycol ditosylate.[29] The decay-corrected radiochemical yield of [^{18}F]-**5** from the tosylate, **8**, was somewhat better over two steps (23%) but with much lower specific activity of 3−6 mCi/μmole (n = 3; Scheme 2). The total time of preparation (radiosynthesis and chromatography and formulation) ranged from 120 to 130 min (125 ± 5 min). Compound **5** has a favorable log $D_{(o/w)}$ of 2.1 ± 0.6 and is highly protein bound in serum (98.5 ± 1.0%) and 1% BSA (99.0 ± 0.3%).

To determine whether compound **5** retains a kinase inhibition profile that is similar to dasatinib, we characterized the inhibition of kinase activity. In vitro and cellular assays demonstrated that

Scheme 2. Two Radiosynthetic Routes to an [^{18}F] Derivative of Dasatinib[a]

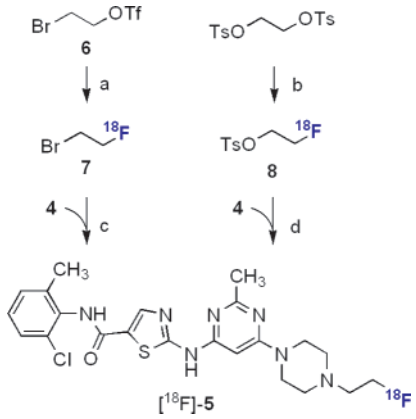

[a] Reagents and conditions: (a) [^{18}F]-KF/Kryptofix 2.2.2, K_2CO_3, *o*-dichlorobenzene, 105 °C, 10 min; (b) [^{18}F]-KF/Kryptofix 2.2.2, K_2CO_3, CH_3CN, 110 °C, 10 min; (c) NaI, $CsCO_3$, 1:1 DMF/CH_3CN, 140 °C, 40 min; (d) DMSO, 160 °C, 30 min.

Table 1. Compound **5** Has Kinase and Cellular Inhibition Characteristics That Are Similar to Dasatinib[a]

	dasatinib IC_{50} (nM)	cmpd **5** IC_{50} (nM)
Abl protein	4.2 ± 0.4	9.1 ± 0.8
Src protein	1.5 ± 1.1	3.5 ± 2.2
K562 cells	1.0 ± 0.2	1.1 ± 0.2
R10 neg cells (M07e/p210$^{bcr-abl}$)	0.07 ± 0.02	0.10 ± 0.02
M07e cells[b]	1.2 ± 0.8	1.1 ± 0.3

[a] Mean of three experiments in each. [b] Grown in 50 ng/mL SCF (Kit ligand).

fluorinated analog **5** has inhibitory activity that closely parallels that of dasatinib. Compound **5** inhibits Abl and Src kinase activity at roughly half the potency of dasatinib in our assays (Table 1).

Compound **5** is equipotent with dasatinib in inhibiting proliferation of cells dependent on Bcr-Abl for growth. K562 growth was inhibited at an IC_{50} of 1.1 nM and M07e/p210$^{bcr-abl}$ cells at 0.10 nM. Also, Kit ligand dependent growth of the parental M07e line was inhibited with an IC_{50} of 1.1 nM. This result correlates well with the strong inhibition of Kit kinase as seen in the kinase panel.

Kinase inhibition by **5** at 10 nM was examined in a panel of 21 kinases, which includes many relevant members for malignancies of interest (Figure 2). As expected, the pattern of kinase binding data for dasatinib[30] is very similar to the kinase inhibition profile of compound **5** (see Table S1). Abl, Src, and Kit are inhibited at >97% at 10 nM, which corresponds to IC_{50} values of <2 nM. Furthermore, **5** potently inhibited Tec kinase and two representative ephrin receptor tyrosine kinases, EphA2 and EphB4. Recently, Tec and Btk kinases were found to be major targets of dasatinib by chemical proteomics.[31] While inhibiting the ephrin receptors may be a double-edged sword for therapeutics due to tumor-suppressor signaling,[32] they are upregulated in a variety of cancers[33] and hold promise in molecular imaging.[34]

While we are particularly interested in potent Src/Abl binding radiotracers, it is obvious that this pharmacophore is not selective and interacts with a number of kinases.[30] A tumor overexpressing a particular kinase, such as Bcr-Abl or Src, can however selectively uptake a high-affinity probe in the presence of surrounding tissues that have negligible kinase expression. We

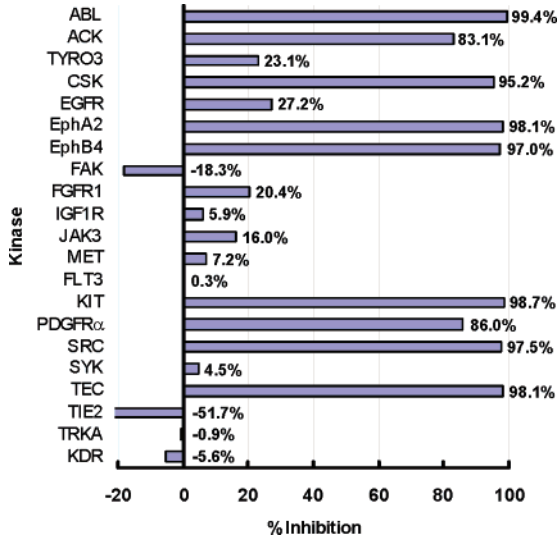

Figure 2. Inhibitory activity of **5** on 21 kinases at 10 nM.

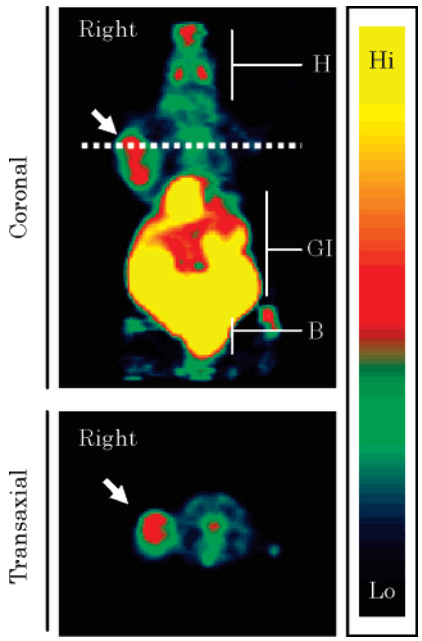

Figure 3. MicroPET imaging of a K562 xenograft in a mouse with [^{18}F]-**5** from 60 to 75 min.

have shown this selective uptake is possible with a related kinase-targeted radiotracer in Bcr-Abl overexpressing K562 cells.[24]

In preliminary in vivo studies in mice, **5** has not shown toxicity at a dose of 0.1 mg/kg. HPLC analysis of plasma samples revealed that [^{18}F]-**5** was metabolized significantly over a 2 h time course (see Table S2).

In Vivo PET Imaging. Preliminary in vivo results have been obtained in three athymic mice bearing subcutaneous K562 (CML) tumor xenografts in the right shoulder. [^{18}F]-**5** (14 ± 1 MBq, 375 ± 25 μCi) was injected through the tail vein and the subjects were imaged in a microPET scanner. Figure 3 shows the microPET scan of one representative mouse 60 min after injection; the exposure time was 15 min. Tracer activity was evident within the tumor xenograft (white arrow) and was determined to be 1.1% of the injected dose by ROI (region of interest) analysis. The coronal image shows [^{18}F]-**5** activity in the tumor, blood pool activity in the head (H), physiologic excretion into the liver and gastrointestinal (GI) tract as well as into the kidneys and bladder (B). The transaxial image was taken

at the level of the known palpable tumor as shown in the coronal section (broken line). The intensity of the radiotracer activity is color-graded as depicted by the colored scale.

There was no significant uptake observed in bone, suggesting that [^{18}F]-**5** did not undergo rapid metabolic defluorination. Instead, the compound appears to be cleared via the hepatobiliary route predominantly. This result correlates with the distribution of dasatinib in mice.

The question remains whether uptake is a function of expression of Bcr-Abl. The expression of Bcr-Abl in K562 can be modulated using siRNAs;[35] further experiments using this approach are underway to determine the correlation between the expression of Bcr-Abl and tumor uptake.

Conclusions

We report the radiosynthesis, biological evaluation, and preliminary in vivo micro-PET imaging of a fluorine-18 radiotracer based on a potent, multitargeted kinase inhibitor, dasatinib, which is approved for the treatment of imatinib-resistant CML and Ph+ ALL. Compound **5** has similar target selectivity to dasatinib in vitro and retains strong antitumor potency. Radiosynthesis of [^{18}F]-**5** was accomplished in a two-step approach by radiofluorination of either 2-bromoethyltriflate or ethylene glycol ditosylate and subsequent alkylation of piperazine precursor **4**. Production runs of [^{18}F]-**5** from 2-bromoethyltriflate had an average specific activity of 2560 mCi/μmol ($n = 11$) in 125 ± 5 min after end-of-bombardment. Probe [^{18}F]-**5** had significant K562 tumor uptake in mice and, thus, is being investigated further as a molecularly targeted PET imaging probe with in vivo models of systemic CML, GIST, and other malignancies involving Abl, Src, and Kit.

Possibly the most exciting potential of kinase-targeted probes like [^{18}F]-**5** is to visualize tumor characteristics on a molecular level, noninvasively, such as the existence or emergence of drug-resistant leukemia in bone marrow. Established proliferative imaging modalities like [^{18}F]-FLT or [^{18}F]-FDG are valuable but cannot give the same information about the molecular changes occurring during disease progression or the emergence of resistance. Our ultimate goal is to determine whether [^{18}F]-**5** is useful in identifying malignancies that might respond to dasatinib treatment and thereby use PET imaging with [^{18}F]-**5** as a prognostic tool for kinase inhibitor therapy.

Experimental Section

Chemistry. Dasatinib, 2. Dasatinib, **2**, was synthesized according to the procedure of Lombardo, et al.[13]

***N*-(2-Chloro-6-methylphenyl)-2-(2-methyl-6-(piperazin-1-yl)-pyrimidin-4-ylamino)thiazole-5-carboxamide, 4.** 2-(6-Chloro-2-methylpyrimidin-4-ylamino)-*N*-(2-chloro-6-methylphenyl)thiazole-5-carboxamide, **3**[13] (1.00 g, 2.54 mmol), piperazine (2.19 g, 25.4 mmol), and *N*,*N*-diisopropylethylamine (0.84 mL, 5.07 mmol) were dissolved in 30 mL of dry 1,4-dioxane and refluxed overnight. The solvent was stripped and the residue was triturated several times with DI water/MeOH, MeOH/ether, and ether. The white solid was dried under high vacuum to give precursor **4** (0.88 g, 78%). ^{1}H NMR (DMSO-d_6) δ 9.85 (s, 1H), 8.20 (s, 1H), 7.39 (dd, 1H, J = 7.5, 1.5 Hz), 7.29 − 7.22 (m, 2H), 6.01 (s, 1H), 3.43 (m, 4H), 2.73 (m, 4H), 2.39 (s, 3H), 2.23 (s, 3H); ^{13}C NMR (DMSO-d_6) δ 165.1, 162.6, 162.5, 159.9, 156.9, 140.8, 138.8, 133.5, 132.4, 129.0, 128.1, 127.0, 125.6, 82.4, 45.3 (2), 44.8 (2), 25.6, 18.3; FTIR (ATR) ν_{max} 3190, 2950, 1619, 1571, 1506, 1410, 1294, 1205, 1185, 769; MS-ESI m/z 445 [M + H]$^+$; HRMS (FAB+) calcd for $C_{20}H_{22}ClN_7OS$, 443.1295; found, 443.1303; HPLC t_R = 2.6 min (Phenomenex Gemini C18 250 × 4.6 mm, 50% 20 mM pH 4.1 KH_2PO_4/50% CH_3CN, 1 mL/min, λ = 254 nm).

***N*-(2-Chloro-6-methylphenyl)-2-(6-(4-(2-fluoroethyl)piperazin-1-yl)-2-methylpyrimidin-4-ylamino)thiazole-5-carboxamide, 5.** Piperazine **4** (50 mg, 0.11 mmol), 1-bromo-2-fluoroethane (21 μL, 0.27 mmol), K_2CO_3 (78 mg, 0.56 mmol), NaI (2 mg, 0.01 mmol), and 5 mL of CH_3CN were added to a 10 mL screw-top tube under argon. The vial was sealed and stirred 2 h at 60 °C. Another 21 μL (0.27 mmol) of 1-bromo-2-fluoroethane was added, and the mixture was stirred another 2 h. The reaction mixture was partitioned between 30 mL of EtOAc and 30 mL water. The organic layer was washed with water and brine, dried over $MgSO_4$, and concentrated to find a yellow oil. Purification by gradient flash chromatography (SiO_2, 0% to 10% 7 N NH_3 in MeOH/CH_2Cl_2) yielded 46 mg (84%) of compound **5**, a white powder: ^{1}H NMR (DMSO-d_6) δ 11.44 (s, 1H), 9.85 (s, 1H), 8.20 (s, 1H), 7.39 (d, 1H, J = 7.0 Hz), 7.27 − 7.24 (m, 2H), 6.04 (s, 1H), 4.62 − 4.48 (dt, 4H, J = 47.8, 4.8 Hz), 3.51 (m, 4H), 2.69 − 2.60 (m, 2H, dt, 4H, J = 28.8, 4.8 Hz), 2.68 (m, 4H) 2.39 (s, 3H), 2.22 (s, 3H); ^{13}C NMR (DMSO-d_6) δ 165.1, 162.5, 162.4, 159.9, 156.9, 140.8, 138.8, 133.5, 132.4, 129.0, 128.1, 127.0, 125.7, 82.6, 81.7 (d, J = 164 Hz), 57.5 (d, J = 19 Hz), 52.4 (2), 43.5 (2), 25.5, 18.3; ^{19}F NMR (DMSO-d_6) δ −217; FTIR (ATR) ν_{max} 3202, 2945, 1622, 1576, 1504, 1413, 1394, 1290, 1188, 768; MS-ESI m/z 490 [M + H]$^+$; HRMS (FAB+) calcd for $C_{22}H_{25}ClFN_7OS$, 489.1514; found, 489.1519; HPLC t_R = 5.6 min (Phenomenex Gemini C18 250 × 4.6 mm, 50% 20 mM pH 4.1 KH_2PO_4/50% CH_3CN, 1 mL/min, λ = 254 nm).

2-Bromoethyltriflate, 6. 2-Bromoethyltriflate, **6**, was produced as in Chi et al., distilled, aliquated, sealed under argon, and stored at −20 °C.[27] ^{1}H NMR ($CDCl_3$) δ 4.75 (t, 2H, J = 6.4 Hz), 3.61 (t, 2H, J = 6.4 Hz); ^{13}C NMR ($CDCl_3$) δ 118.5 (q, J = 320 Hz), 74.2, 26.1; ^{19}F NMR ($CDCl_3$) δ −75.0.

Radiosynthesis. [^{18}F]-*N*-(2-Chloro-6-methylphenyl)-2-(6-(4-(2-fluoroethyl)piperazin-1-yl)-2-methylpyrimidin-4-ylamino)thiazole-5-carboxamide, [^{18}F]-5. The radiosynthesis of [^{18}F]-**5** was performed via two methods from 2-bromoethyltriflate, **6** (method A) or ethylene glycol ditosylate (method B; Supporting Information). Routine production of [^{18}F]-**5** currently uses method A.

Method A. The QMA cartridge containing cyclotron-produced [^{18}F] fluoride ion was eluted with a solution containing 420 μL of H_2O and 120 μL of 0.25 M K_2CO_3 into a 10 mL Reacti-vial containing 15 mg of Kryptofix [2.2.2] (4,7,13,16,21,24-hexaoxa-1,10-diazabicyclo[8.8.8]hexacosane) in 1.0 mL of CH_3CN. Water was removed azeotropically with CH_3CN (3 × 1.0 mL) at 100−105 °C. The Reacti-vial was cooled to 0 °C, and to the anhydrous [^{18}F] KF/K_2CO_3 complexed with Kryptofix was added a solution of 2-bromoethyltriflate, **6**, (0.054 mmole) in *o*-dichlorobenzene (500 μL) and heated to 105 °C for 10 min. The [^{18}F]-1-bromo-2-fluoroethane ([^{18}F]-**7**) formed was distilled at 120 °C by bubbling a stream of argon (100 mL/min) into another Reacti-Vial maintained at −25 °C, containing a solution of piperazine precursor **4** (6.5 mg, 14.6 μM), NaI (9.0 mg, 60 μM), and Cs_2CO_3 (5 mg, 15.3 μM) in 500 μL of 1:1 CH_3CN:DMF. The activity in the receiving vial was measured periodically to follow the distillation procedure (5 min). The Reacti-Vial was fitted with a new, unpierced septum to minimize loss of [^{18}F]-**7** at high temperature. The solution was heated to 120 °C for 40 min, cooled, diluted with 1.2 mL of 1:4 CH_3CN/50 mM pH 5.5 NaOAc and passed through a 13 mm syringe filter (0.25 μm). This solution was injected onto a C_{18} semipreparative HPLC column and eluted under gradient conditions; 80%A (50 mM pH 5.5 NaOAc)/20% B (CH_3CN) to 20% A/80% B. [^{18}F]-**5** eluted at 15.3 min, which was well resolved from precursor **4** (t_R = 13.4 min). For intravenous administration, the product-containing fraction was stripped of solvent by rotary evaporation, formulated in 5% BSA in saline to the proper dosage and sterile filtered. The radiochemical purity of the final formulation was confirmed using analytical HPLC. Coelution with nonradioactive ^{19}F reference compound **5** confirmed the identity of the radiotracer. To measure radiochemical and chemical purity (>99%), [^{18}F]-**5** was reinjected from the semi-prep HPLC product peak on analytical HPLC (product t_R = 13.2 min, isocratic 60% 50 mM

pH 5.5 NaOAc/40% CH_3CN, 1.0 mL/min). An example of this chromatogram appears in the Supporting Information (Figure S2). Total time of radiosynthesis was 120 ± 5 minutes from EOB. The decay-corrected radiochemical yields ($n = 3$) were 25.1 ± 5.8% from [^{18}F]-1-bromo-2-fluoroethane and 6.6 ± 2.3% overall from starting [^{18}F]-fluoride. The specific activity ranged from 108−7350 mCi/μmol (average 2560 mCi/μmol, $n = 11$).

Acknowledgment. The authors thank the U.S. Department of Energy for support under Contract Nos. DE-FG02-86ER60407 and ER63693 and the National Institutes of Health under Contract Nos. P50 CA86438 and P30 CA008748. Technical services provided by the MSKCC Small-Animal Imaging Core Facility, supported in part by NIH Small-Animal Imaging Research Program (SAIRP) Grant No. R24 CA83084 and NIH Center Grant No. P30 CA08748, are gratefully acknowledged. D.R.V. and B.C. also thank the MeadWestvaco Corp. for their continuing support and the Kirin Brewery Co., Ltd. (Tokyo, Japan) for rhGM-CSF and rhSCF.

Supporting Information Available: Experimental details of general synthesis, molecular modeling, protein binding, log $D_{o/w}$ determination, kinase assays, cell proliferation assays, metabolite analysis, and mouse PET imaging. This material is available free of charge via the Internet at http://pubs.acs.org.

References

(1) Hicks, R. J. The role of PET in monitoring therapy. *Cancer Imaging* **2005**, *5*, 51−57.
(2) Shields, A. F. Positron emission tomography measurement of tumor metabolism and growth: Its expanding role in oncology. *Mol. Imaging Biol.* **2006**, *8*, 141−150.
(3) Hernandez, S. E.; Krishnaswami, M.; Miller, A. L.; Koleske, A. J. How do Abl family kinases regulate cell shape and movement? *Trends Cell Biol.* **2004**, *14*, 36−44.
(4) Wang, J. Y. Regulation of cell death by the Abl tyrosine kinase. *Oncogene* **2000**, *19*, 5643−5650.
(5) Wong, S.; Witte, O. N. The BCR-ABL story: Bench to bedside and back. *Annu. Rev. Immunol.* **2004**, *22*, 247−306.
(6) Chen, T.; George, J. A.; Taylor, C. C. Src tyrosine kinase as a chemotherapeutic target: Is there a clinical case? *Anticancer Drugs* **2006**, *17*, 123−131.
(7) Deininger, M.; Buchdunger, E.; Druker, B. J. The development of imatinib as a therapeutic agent for chronic myeloid leukemia. *Blood* **2005**, *105*, 2640−2653.
(8) Zimmermann, J.; Buchdunger, E.; Mett, H.; Meyer, T.; Lydon, N. B. Potent and selective inhibitors of the Abl-kinase: Phenylamino-pyrimidine (PAP) derivatives. *Bioorg. Med. Chem. Lett.* **1997**, *7*, 187−192.
(9) Hornick, J. L.; Fletcher, C. D. The role of KIT in the management of patients with gastrointestinal stromal tumors. *Hum. Pathol.* **2007**, *38*, 679−687.
(10) Melo, J. V.; Chuah, C. Resistance to imatinib mesylate in chronic myeloid leukaemia. *Cancer Lett.* **2007**, *249*, 121−132.
(11) Tauchi, T.; Ohyashiki, K. The second generation of BCR-ABL tyrosine kinase inhibitors. *Int. J. Hematol.* **2006**, *83*, 294−300.
(12) Weisberg, E.; Manley, P. W.; Cowan-Jacob, S. W.; Hochhaus, A.; Griffin, J. D. Second generation inhibitors of BCR-ABL for the treatment of imatinib-resistant chronic myeloid leukaemia. *Nat. Rev. Cancer* **2007**, *7*, 345−356.
(13) Lombardo, L. J.; Lee, F. Y.; Chen, P.; Norris, D.; Barrish, J. C.; Behnia, K.; Castaneda, S.; Cornelius, L. A. M.; Das, J.; Doweyko, A. M.; Fairchild, C.; Hunt, J. T.; Inigo, I.; Johnston, K.; Kamath, A.; Kan, D.; Klei, H.; Marathe, P.; Pang, S. H.; Peterson, R.; Pitt, S.; Schieven, G. L.; Schmidt, R. J.; Tokarski, J.; Wen, M. L.; Wityak, J.; Borzilleri, R. M. Discovery of *N*-(2-chloro-6-methylphenyl)-2-(6-(4-(2-hydroxyethyl)-piperazin-1-yl)-2-methylpyrimidin-4-ylamino)thiazole-5-carboxamide (BMS-354825), a dual Src/Abl kinase inhibitor with potent antitumor activity in preclinical assays. *J. Med. Chem.* **2004**, *47*, 6658−6661.
(14) Shah, N. P.; Tran, C.; Lee, F. Y.; Chen, P.; Norris, D.; Sawyers, C. L. Overriding imatinib resistance with a novel ABL kinase inhibitor. *Science* **2004**, *305*, 399−401.
(15) Abourbeh, G.; Dissoki, S.; Jacobson, O.; Litchi, A.; Ben Daniel, R.; Laki, D.; Levitzki, A.; Mishani, E. Evaluation of radiolabeled ML04, a putative irreversible inhibitor of epidermal growth factor receptor, as a bioprobe for PET imaging of EGFR-overexpressing tumors. *Nucl. Med. Biol.* **2007**, *34*, 55−70.
(16) Johnstrom, P.; Fredriksson, A.; Thorell, J. O.; Stone-Elander, S. Synthesis of [methoxy-C-11]PD153035, a selective EGF receptor tyrosine kinase inhibitor. *J. Labelled Compd. Radiopharm.* **1998**, *41*, 623−629.
(17) Lim, J. K.; Negash, K.; Hanrahan, S. M.; VanBrocklin, H. F. Synthesis of 4-(3′-[I-125]iodoanilino)-6,7-dialkoxyquinazolines: Radiolabeled epidermal growth factor receptor tyrosine kinase inhibitors. *J. Labelled Compd. Radiopharm.* **2000**, *43*, 1183−1191.
(18) Wang, J. Q.; Gao, M.; Miller, K. D.; Sledge, G. W.; Zheng, Q. H. Synthesis of [11C]Iressa as a new potential PET cancer imaging agent for epidermal growth factor receptor tyrosine kinase. *Bioorg. Med. Chem. Lett.* **2006**, *16*, 4102−4106.
(19) Wang, J. Q.; Miller, K. D.; Sledge, G. W.; Zheng, Q. H. Synthesis of [18F]SU11248, a new potential PET tracer for imaging cancer tyrosine kinase. *Bioorg. Med. Chem. Lett.* **2005**, *15*, 4380−4384.
(20) Larson, S. M.; Nelp, W. B. The radiocolloid bone marrow scan in malignant disease. *J. Surg. Oncol.* **1971**, *3*, 685−697.
(21) Shreeve, W. W. Use of isotopes in the diagnosis of hematopoietic disorders. *Exp. Hematol.* **2007**, *35*, 173−179.
(22) Agool, A.; Schot, B. W.; Jager, P. L.; Vellenga, E. 18F-FLT PET in hematologic disorders: A novel technique to analyze the bone marrow compartment. *J. Nucl. Med.* **2006**, *47*, 1592−1598.
(23) Ackermann, U.; Tochon-Danguy, H. J.; Nerrie, M.; Nice, E. C.; Sachinidis, J. I.; Scott, A. M. Synthesis, C-11 labeling and biological properties of derivatives of the tyrphostin AG957. *Nucl. Med. Biol.* **2005**, *32*, 323−328.
(24) Veach, D. R.; Namavari, M.; Beresten, T.; Balatoni, J.; Minchenko, M.; Djaballah, H.; Finn, R. D.; Clarkson, B.; Gelovani, J. G.; Bornmann, W. G.; Larson, S. M. Synthesis and in vitro examination of [I-124]-, [I-125]- and [I-131]-2-(4-iodophenylamino) pyrido[2,3-*d*]pyrimidin-7-one radiolabeled Abl kinase inhibitors. *Nucl. Med. Biol.* **2005**, *32*, 313−321.
(25) Kil, K.; Ding, Y.; Lin, K.; Alexoff, D.; Kim, S. W.; Shea, C.; Xu, Y.; Muench, L.; Fowler, J. S. Synthesis and positron emission tomography studies of carbon-11-labeled imatinib (Gleevec). *Nucl. Med. Biol.* **2007**, *34*, 153−163.
(26) Tokarski, J. S.; Newitt, J. A.; Chang, C. Y. J.; Cheng, J. D.; Wittekind, M.; Kiefer, S. E.; Kish, K.; Lee, F. Y. F.; Borzillerri, R.; Lombardo, L. J.; Xie, D. L.; Zhang, Y. Q.; Klei, H. E. The structure of dasatinib (BMS-354825) bound to activated ABL kinase domain elucidates its inhibitory activity against imatinib-resistant ABL mutants. *Cancer Res.* **2006**, *66*, 5790−5797.
(27) Chi, D. Y.; Kilbourn, M. R.; Katzenellenbogen, J. A.; Welch, M. J. A rapid and efficient method for the fluoroalkylation of amines and amides—development of a method suitable for incorporation of the short-lived positron emitting radionuclide F-18. *J. Org. Chem.* **1987**, *52*, 658−664.
(28) Nagar, B.; Hantschel, O.; Young, M. A.; Scheffzek, K.; Veach, D.; Bornmann, V.; Clarkson, B.; Superti-Furga, G.; Kuriyan, J. Structural basis for the autoinhibition of c-Abl tyrosine kinase. *Cell* **2003**, *112*, 859−871.
(29) Block, D.; Coenen, H. H.; Stocklin, G. The nca nucleophilic F-18 fluorination of 1,*N*-disubstituted alkanes as fluoroalkylation agents. *J. Labelled Compd. Radiopharm.* **1987**, *24*, 1029−1042.
(30) Carter, T. A.; Wodicka, L. M.; Shah, N. P.; Velasco, A. M.; Fabian, M. A.; Treiber, D. K.; Milanov, Z. V.; Atteridge, C. E.; Biggs, W. H.; Edeen, P. T.; Floyd, M.; Ford, J. M.; Grotzfeld, R. M.; Herrgard, S.; Insko, D. E.; Mehta, S. A.; Patel, H. K.; Pao, W.; Sawyers, C. L.; Varmus, H.; Zarrinkar, P. P.; Lockhart, D. J. Inhibition of drug-resistant mutants of ABL, KIT, and EGF receptor kinases. *Proc. Natl. Acad. Sci. U.S.A.* **2005**, *102*, 11011−11016.
(31) Hantschel, O.; Rix, U.; Schmidt, U.; Burckstummer, T.; Kneidinger, M.; Schutze, G.; Colinge, J.; Bennett, K. L.; Ellmeier, W.; Valent, P.; Superti-Furga, G. The Btk tyrosine kinase is a major target of the Bcr-Abl inhibitor dasatinib. *Proc. Natl. Acad. Sci. U.S.A.* **2007**, *104*, 13283−13288.
(32) Wang, J. Y. Eph tumour suppression: The dark side of Gleevec. *Nat. Cell Biol.* **2006**, *8*, 785−786.
(33) Noren, N. K.; Pasquale, E. B. Paradoxes of the EphB4 receptor in cancer. *Cancer Res.* **2007**, *67*, 3994−3997.
(34) Cai, W.; Ebrahimnejad, A.; Chen, K.; Cao, Q.; Li, Z.-B.; Tice, D. A.; Chen, X. Quantitative radioimmunoPET imaging of EphA2 in tumor-bearing mice. *Eur. J. Nucl. Med. Mol. Imaging* **2007**, (published online Aug 3, 2007) doi:10.1007/s00259-007-0503-5.
(35) Baker, B. E.; Kestler, D. P.; Ichiki, A. T. Effects of siRNAs in combination with Gleevec on K-562 cell proliferation and Bcr-Abl expression. *J. Biomed. Sci.* **2006**, *13*, 499−507.

JM070342G